iScience, Volume *26*

Supplemental information

Amnion responses to intrauterine inflammation and effects of inhibition of TNF signaling in preterm Rhesus macaque

Pietro Presicce, Monica Cappelletti, Marco Morselli, Feiyang Ma, Paranthaman Senthamaraikannan, Giulia Protti, Brian B. Nadel, Laila Aryan, Mansoureh Eghbali, Lukasz Salwinski, Neema Pithia, Emily De Franco, Lisa A. Miller, Matteo Pellegrini, Alan H. Jobe, Claire A. Chougnet, and Suhas G. Kallapur

Figure S1.

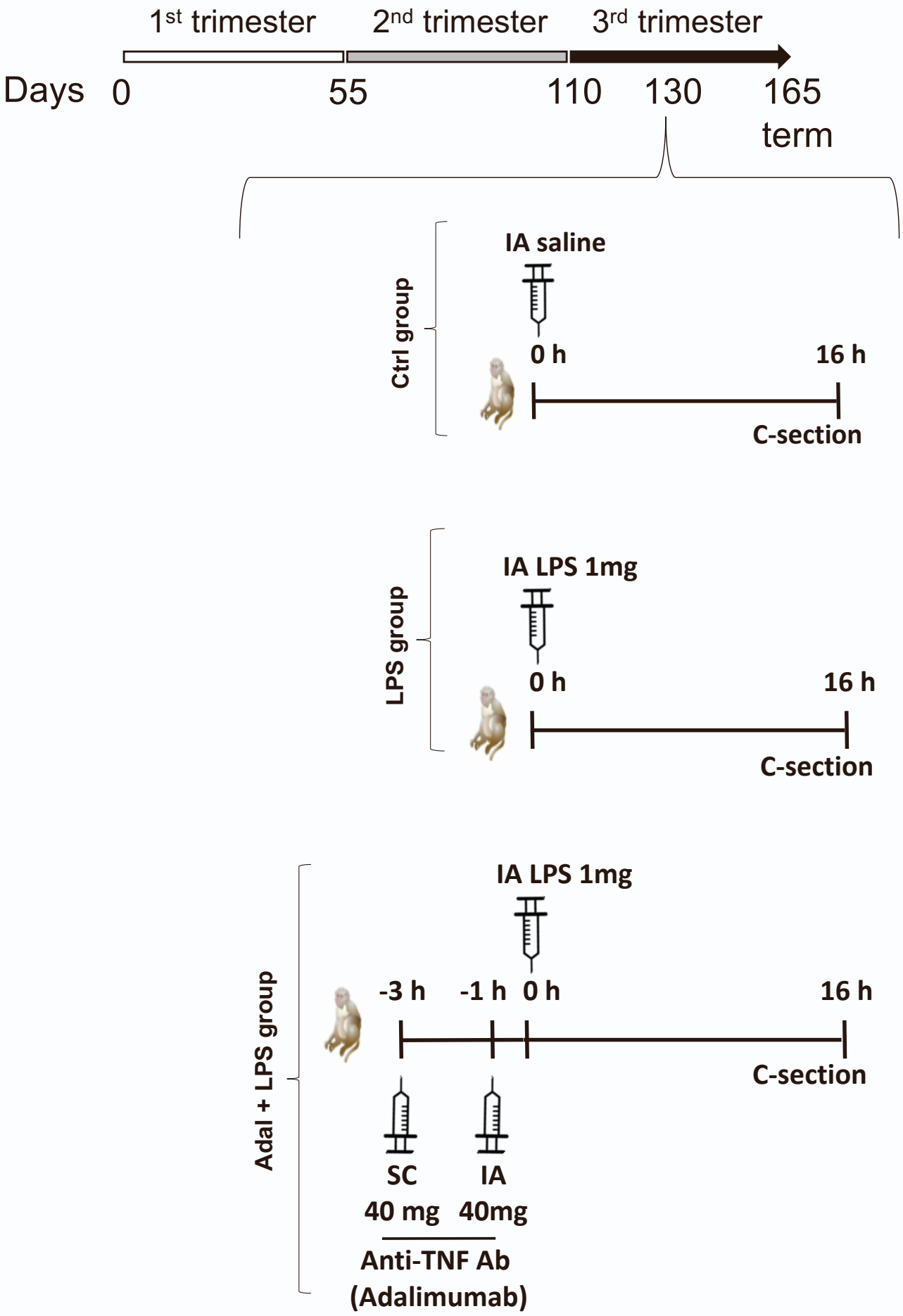
1st trimester
2nd trimester
3rd trimester
Days
0
55
110
130
165
term
Ctrl group
IA saline
0 h
16 h
C-section
LPS group
IA LPS 1mg
0 h
16 h
C-section
Adal + LPS group
IA LPS 1mg
-3 h
-1 h
0 h
16 h
C-section
SC
IA
40 mg
40mg
Anti-TNF Ab
(Adalimumab)

Figure S1. [Experimental design], Related to Figures 1 and 2. Scheme showing the experimental design in the three groups of animals: saline (Ctrl; n=12), LPS- (n=15) and Adalimumab (Adal) + LPS-exposed animals (n=6) (IA=intra-amniotic; SC=sub-cutaneous). One animal belonging to control group received saline by an intramuscular injection.

Figure S2.

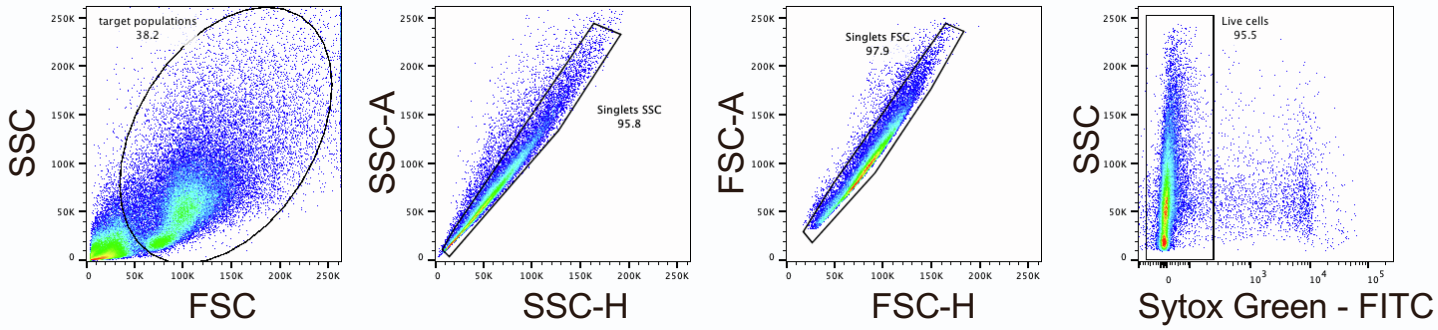

Figure S2. [Flow cytometry gating strategy], Related to Figure 4. Representative gating strategy (n=8) used to isolate live Rhesus chorioamnion-decidua (CAD) cells used for scRNA-seq. Debris were first excluded by SSC and FSC. Doublets were excluded by SSC-H and FSC-H and live cells were finally sorted as Sytox green- cells.

Figure S3.

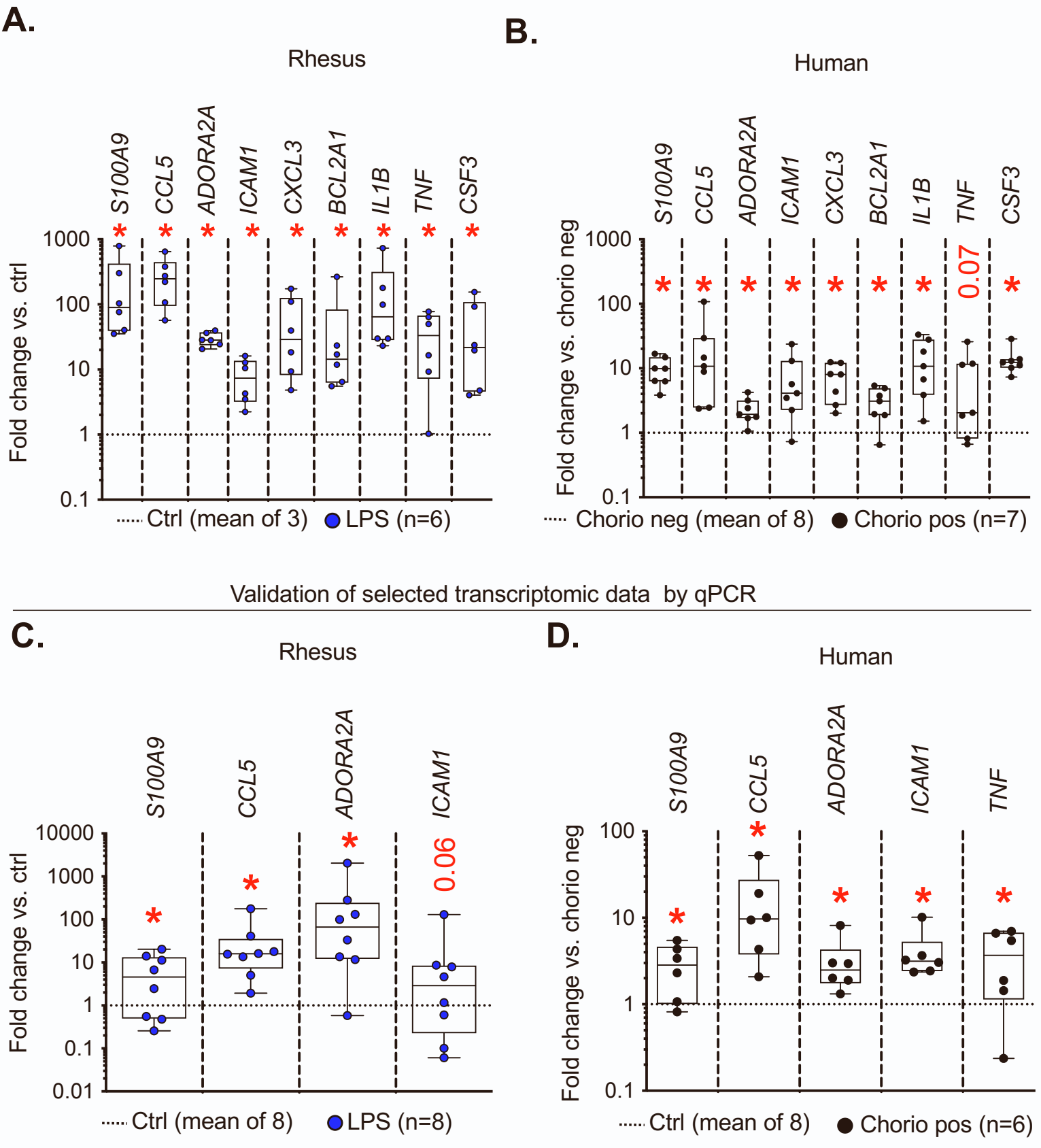
A.
Rhesus
S100A9
CCL5
ADORA2A
ICAM1
CXCL3
BCL2A1
IL1B
TNF
CSF3
Fold change vs. ctrl
1000
100
10
1
0.1
Ctrl (mean of 3)
LPS (n=6)
B.
Human
Fold change vs. chorio neg
0.07
Chorio neg (mean of 8)
Chorio pos (n=7)
Validation of selected transcriptomic data by qPCR
C.
Rhesus
10000
0.01
0.06
Ctrl (mean of 8)
LPS (n=8)
D.
Human
Chorio pos (n=6)

Figure S3. [GO terms associated with inflammation], Related to Figure 2. Bulk RNA-seq expression level of representative genes associated with the biological processes induced by LPS in (A) Rhesus and induced by chorioamnionitis in (B) human is shown as fold change relative to the average value of Ctrl or chorio neg (dashed line). Validation of selected transcript expression by qPCR analysis in (C) Rhesus and (D) human. The values were first internally normalized to the endogenous 18S RNA, and the box plot show fold-change of gene expression normalized to Ctrl in Rhesus or chorio neg in human. Data are represented as mean±SE. P * <0.05 vs. Ctrl in Rhesus or chorio neg in human (Mann–Whitney U test).

Figure S4.

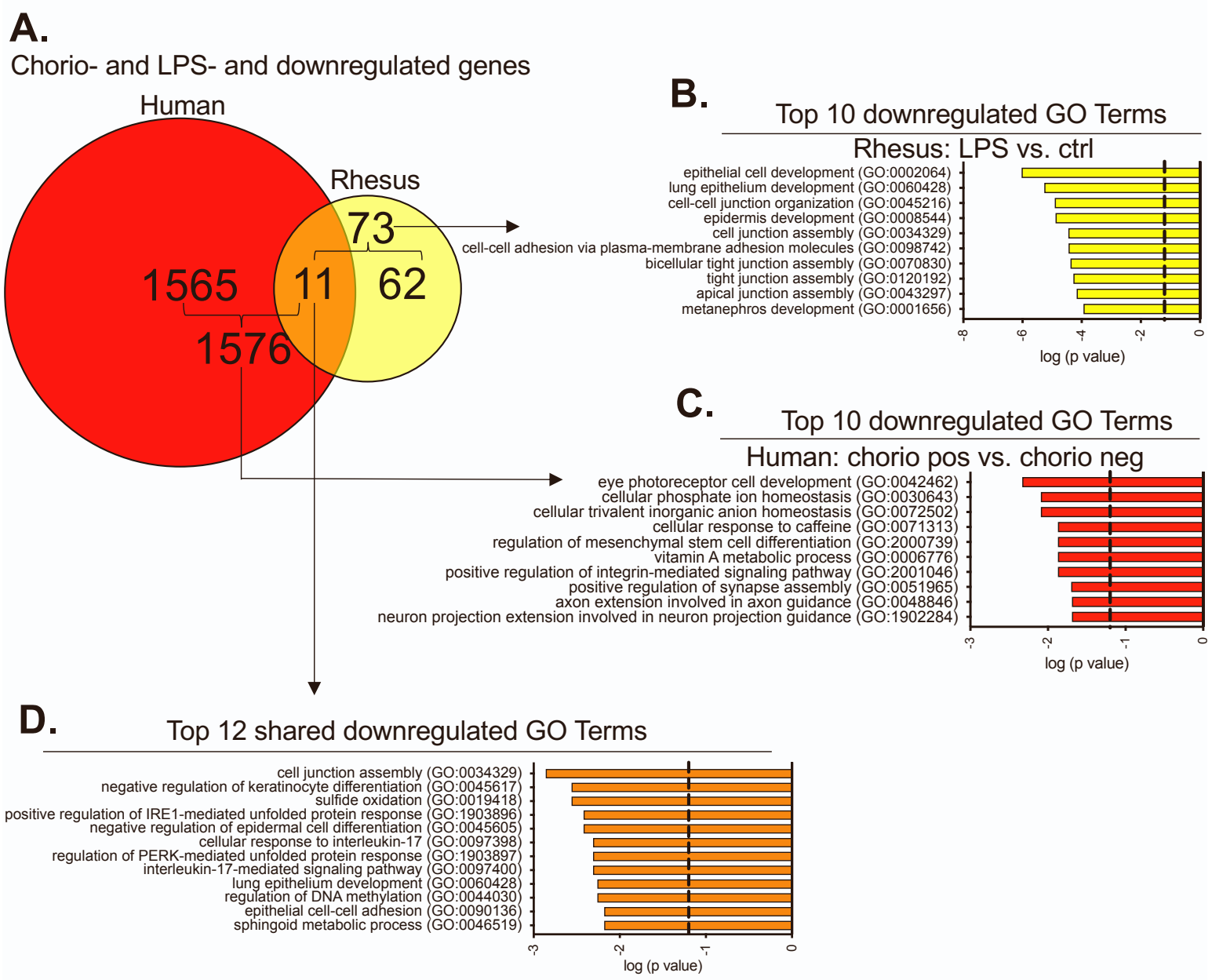

Figure S4. [Downregulated genes upon inflammation in both Rhesus and human], Related to Figure 1. (A) Venn diagrams displaying the genes that were significantly downregulated by chorioamnionitis in human and LPS-exposure in Rhesus (DEGs > 2-fold change; FDR adj p-value<0.05). (B-C) Top 10 GO terms of 73 downregulated genes in Rhesus upon LPS-exposure and of 1576 downregulated human genes upon chorioamnionitis, respectively. (D) Top 12 common downregulated GO terms of the 11 common genes downregulated by inflammation in both Rhesus and human.

Figure S5.

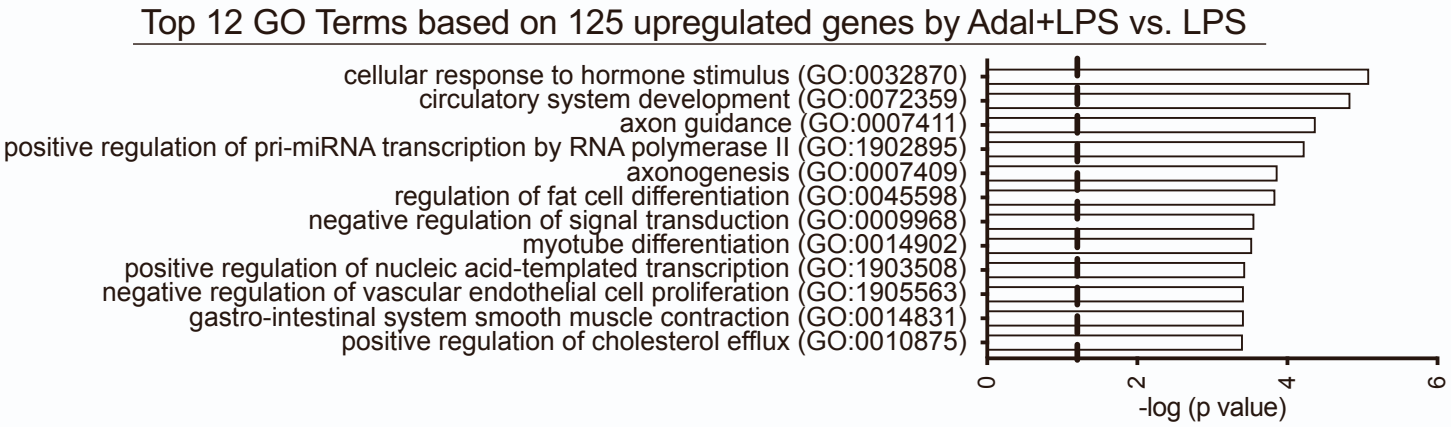

Figure S5. [Upregulated GO terms induced by Adalimumab], Related to Figure 2. Top 12 GO terms of 125 upregulated genes (DEGs > 2-fold change; and FDR adjusted p-value<0.05).

Figure S6.

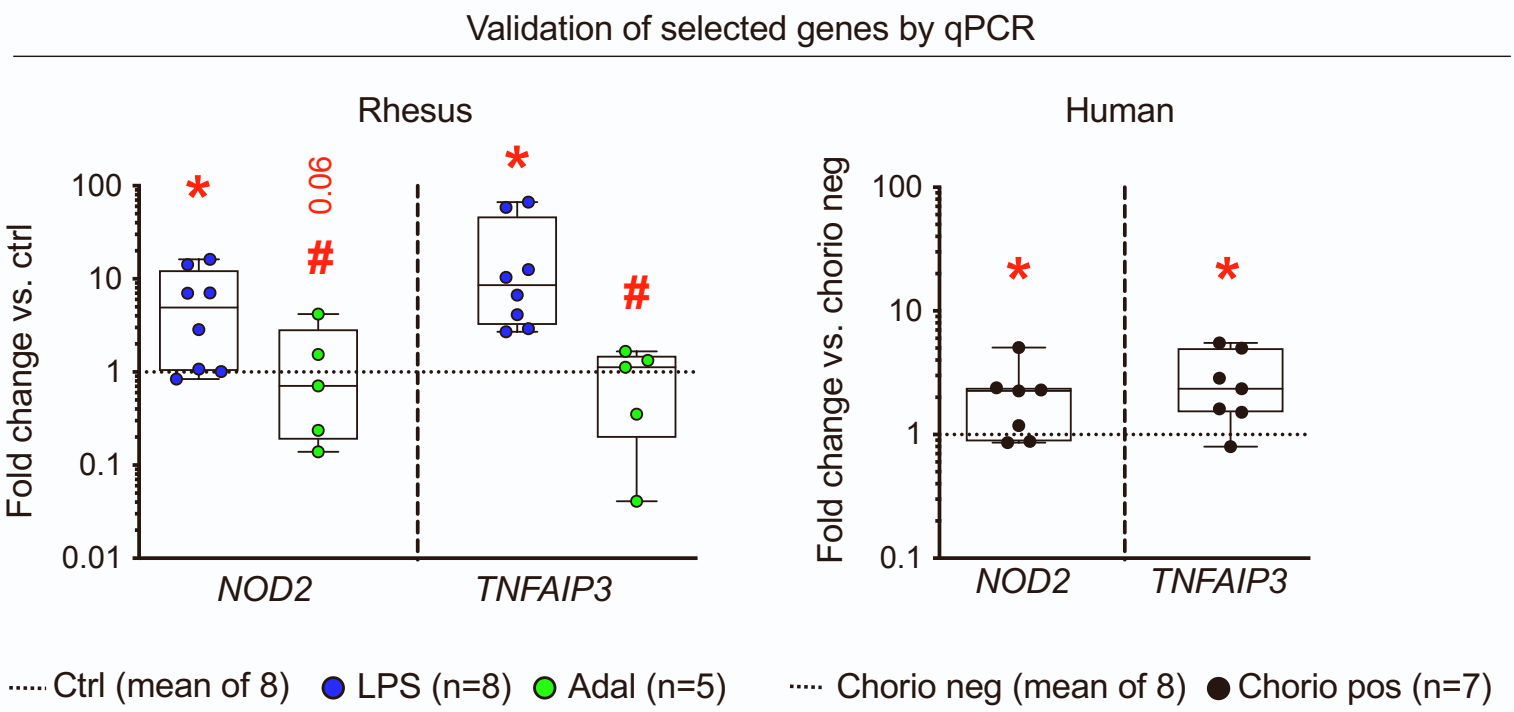

Figure S6. [RNA-seq analysis validation], Related to Figure 3. Validation of selected transcript expression by qPCR analysis in Rhesus and human amnion. qPCR was performed using Rhesus- and human-specific Taqman probes. The values were first internally normalized to the endogenous 18S RNA, and the box plot show fold-change of gene expression normalized to Ctrl in Rhesus or chorio neg in human. Data are represented as mean±SE. P * <0.05 vs. Ctrl in Rhesus or chorio neg in human (Mann–Whitney U test).

Figure S7.

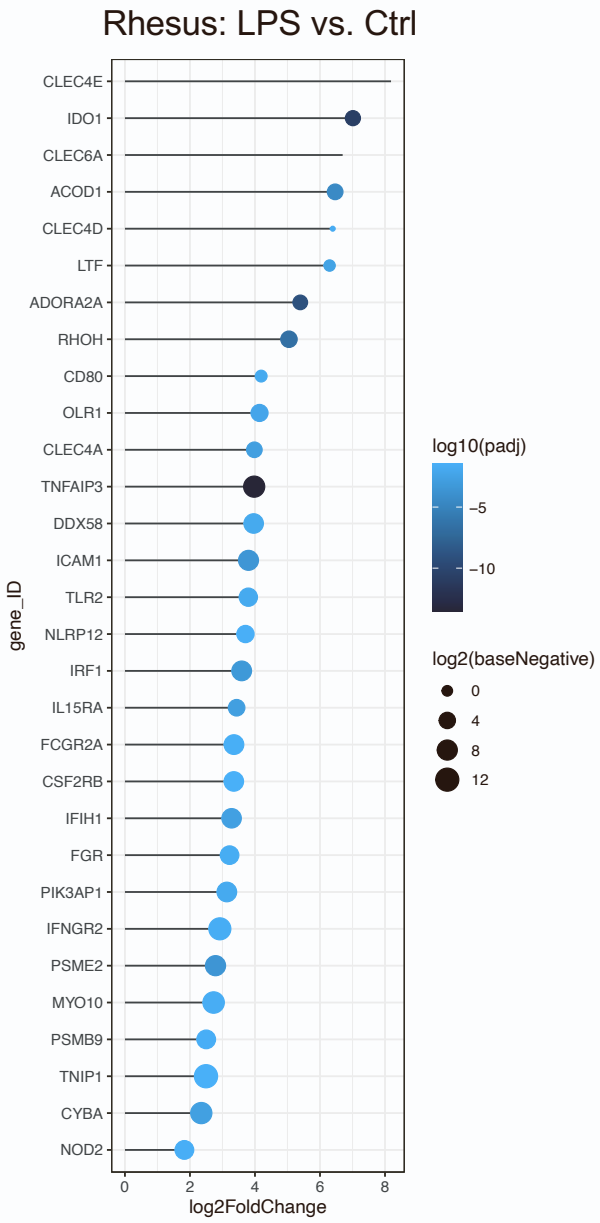
Rhesus: LPS vs. Ctrl
CLEC4E
IDO1
CLEC6A
ACOD1
CLEC4D
LTF
ADORA2A
RHOH
CD80
OLR1
CLEC4A
TNFAIP3
DDX58
ICAM1
TLR2
NLRP12
IRF1
IL15RA
FCGR2A
CSF2RB
IFIH1
FGR
PIK3AP1
IFNGR2
PSME2
MYO10
PSMB9
TNIP1
CYBA
NOD2
gene_ID
0
2
4
6
8
log2FoldChange
log10(padj)
−5
−10
log2(baseNegative)
0
4
8
12

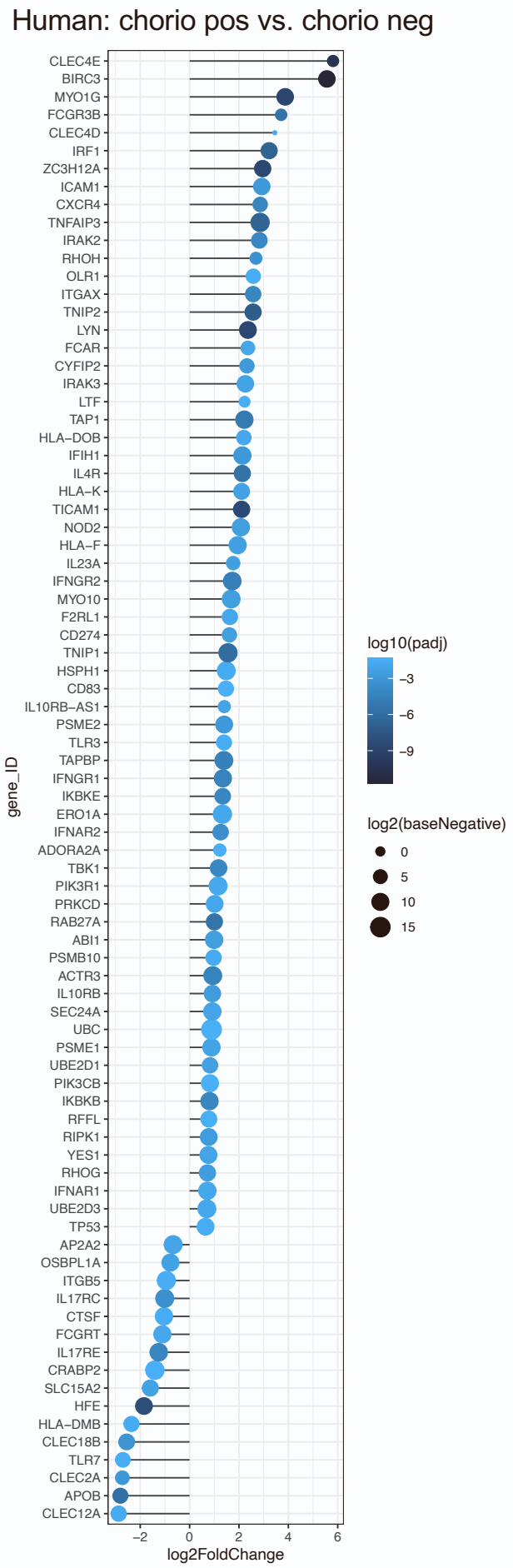
Human: chorio pos vs. chorio neg
CLEC4E
BIRC3
MYO1G
FCGR3B
CLEC4D
IRF1
ZC3H12A
ICAM1
CXCR4
TNFAIP3
IRAK2
RHOH
OLR1
ITGAX
TNIP2
LYN
FCAR
CYFIP2
IRAK3
LTF
TAP1
HLA−DOB
IFIH1
IL4R
HLA−K
TICAM1
NOD2
HLA−F
IL23A
IFNGR2
MYO10
F2RL1
CD274
TNIP1
HSPH1
CD83
IL10RB−AS1
PSME2
TLR3
TAPBP
IFNGR1
IKBKE
ERO1A
IFNAR2
ADORA2A
TBK1
PIK3R1
PRKCD
RAB27A
ABI1
PSMB10
ACTR3
IL10RB
SEC24A
UBC
PSME1
UBE2D1
PIK3CB
IKBKB
RFFL
RIPK1
YES1
RHOG
IFNAR1
UBE2D3
TP53
AP2A2
OSBPL1A
ITGB5
IL17RC
CTSF
FCGRT
IL17RE
CRABP2
SLC15A2
HFE
HLA−DMB
CLEC18B
TLR7
CLEC2A
APOB
CLEC12A
gene_ID
−2
0
2
4
6
log2FoldChange
log10(padj)
−3
−6
−9
log2(baseNegative)
0
5
10
15

Figure S7. [Expression of innate immune genes in the amnion exposed to inflammation], Related to Figure 6. Lollipop chart from bulk RNA-seq data showing fold change and significance of several innate immune genes both in the Rhesus exposed to LPS vs. Ctrl and human chorio pos vs. chorio neg. Color intensity corresponds to log adjusted p-value and the size of the dot corresponds to log 2-fold increase relative to no inflammation group. The gene markers were curated from the corresponding GO terms 2001188, 0019884, 0019883, 0019882, 0002504, 0019885, 001986, 0042590, and 0002491.

Figure S8.

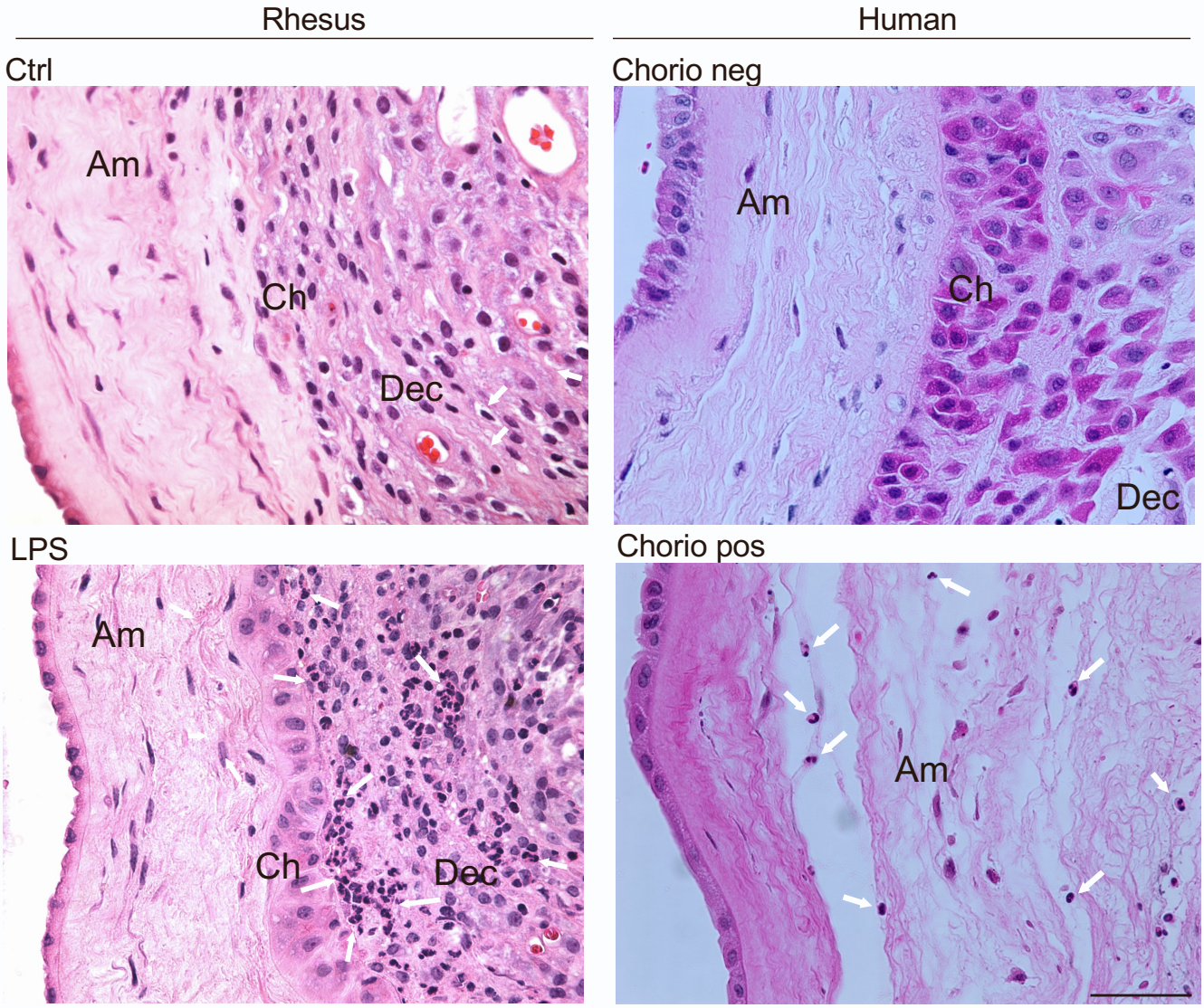

Figure S8. [Immune cell infiltration in fetal membranes exposed to chorioamnionitis], Related to Figures 1 and 2. Representative pictures of fixed membranes paraffin embedded showing Amnion (Am), Chorion (Ch), and Decidua parietalis (Dec). White arrows show neutrophil infiltration. Note that the neutrophil infiltration is restricted to chorio-decidua interface in LPS-exposed Rhesus macaques, while it is present in the amnion of 5 out of 7 human chorioamnionitis samples. No neutrophils were seen in Ctrl Rhesus or chorio neg human membranes. Bar = 50 μm

Figure S9.

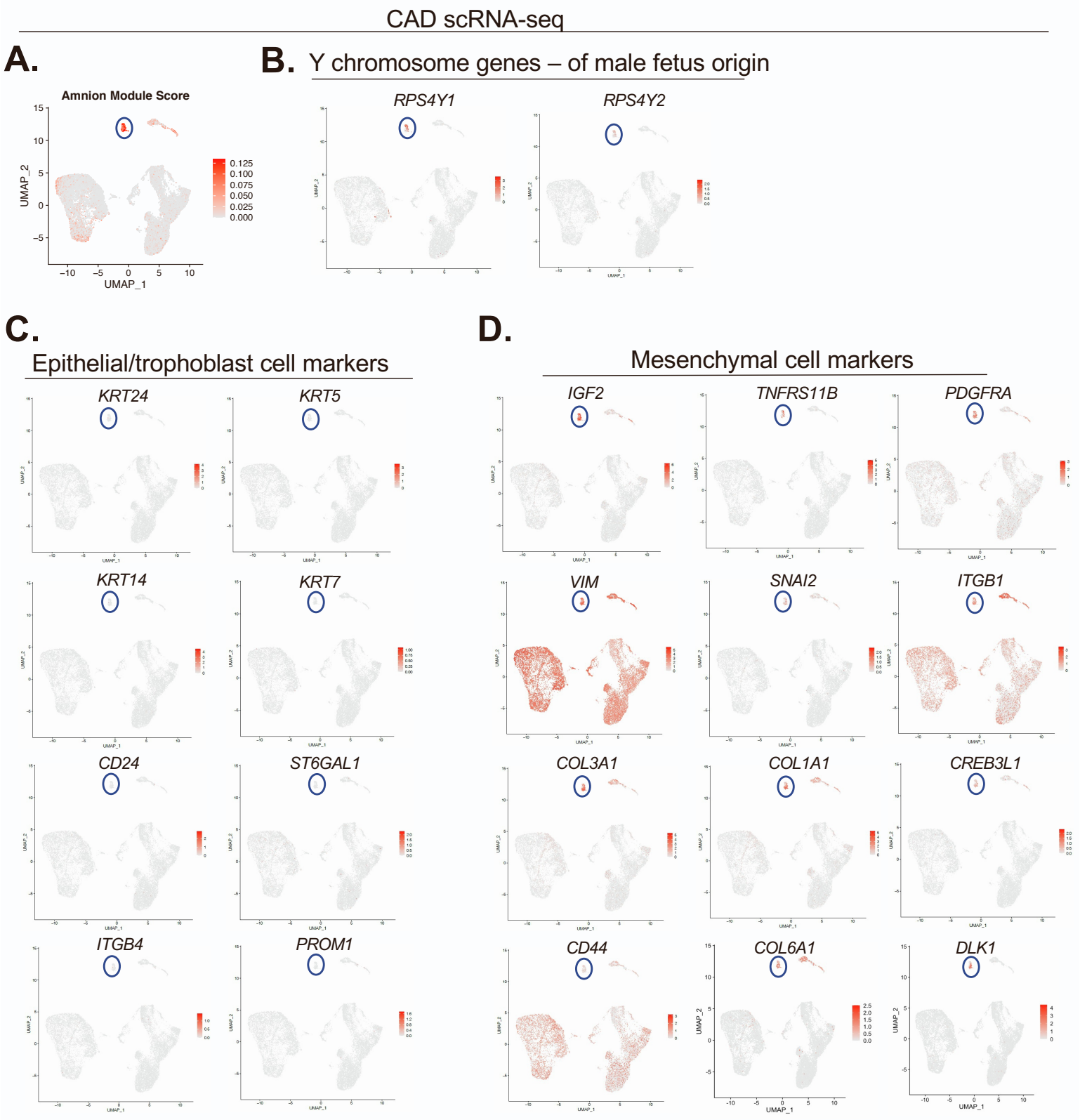

Figure S9. [Annotation of amnion mesenchymal amnion cells (AMC) in the scRNA-seq of chorioamnion-decidua (CAD)], Related to Figure 4. UMAP projection of the CAD cells is shown as in Figure 4A. (A) Top 100 genes expressed in the bulk RNA-seq of dissected human amnion with the highest proportional median from Kim et al., 2012. (B) Male fetal expression of Y chromosome genes RPS4Y1 and RPS4Y2 were limited to the AMCs and a few other choriodecidual cells. (C) Epithelial/trophoblast cell markers were not expressed in the AMCs. (D) Mesenchymal cell markers were predominantly expressed in the AMCs. (Ctrl n=1; LPS n=3; Adal+LPS n=3). The AMC cluster is outlined by a blue oval.

Figure S10.

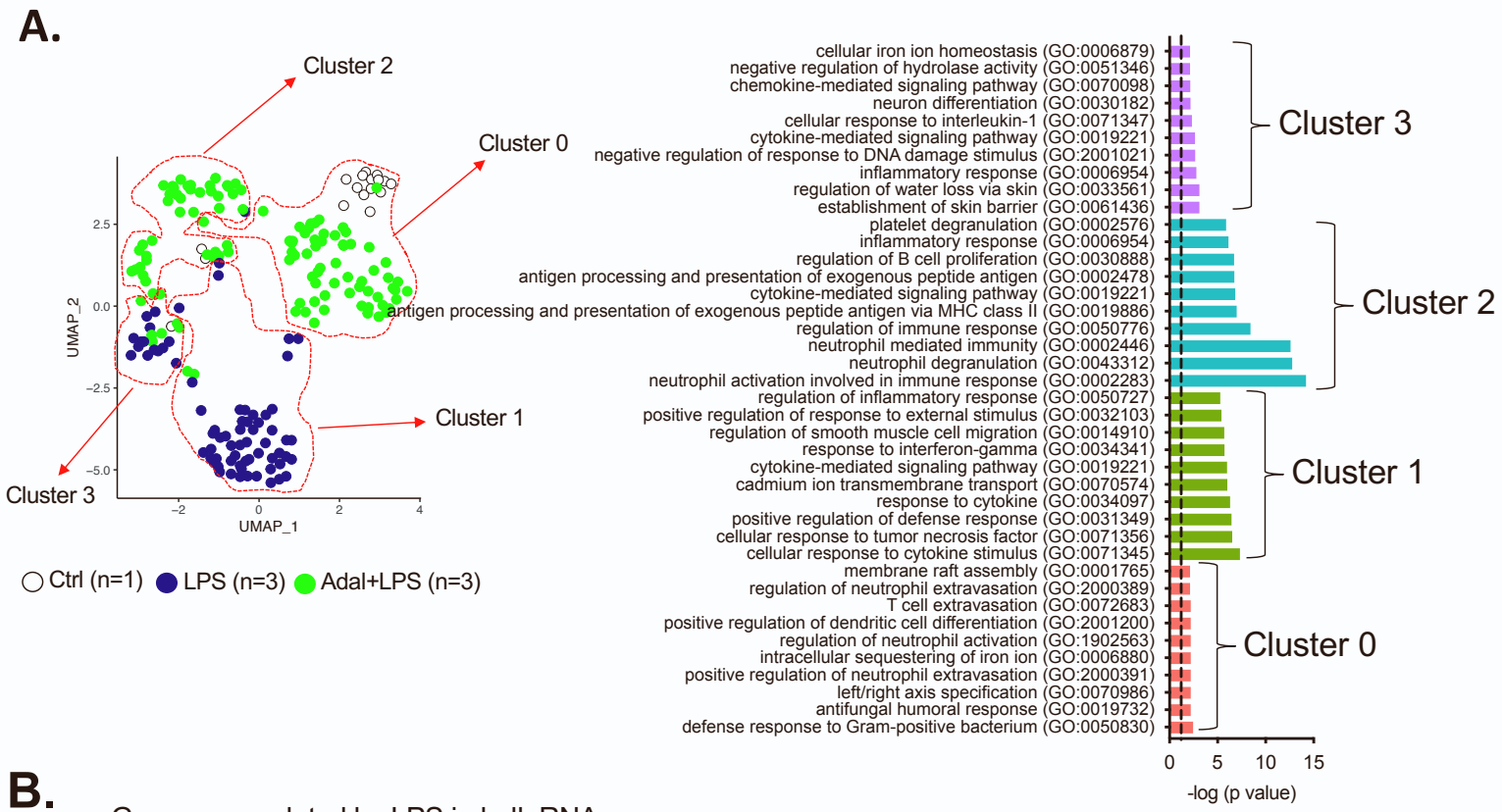
A.
Cluster 2
Cluster 0
Cluster 1
Cluster 3
UMAP_2
UMAP_1
Ctrl (n=1)
LPS (n=3)
Adal+LPS (n=3)
cellular iron ion homeostasis (GO:0006879)
negative regulation of hydrolase activity (GO:0051346)
chemokine-mediated signaling pathway (GO:0070098)
neuron differentiation (GO:0030182)
cellular response to interleukin-1 (GO:0071347)
cytokine-mediated signaling pathway (GO:0019221)
negative regulation of response to DNA damage stimulus (GO:2001021)
inflammatory response (GO:0006954)
regulation of water loss via skin (GO:0033561)
establishment of skin barrier (GO:0061436)
platelet degranulation (GO:0002576)
inflammatory response (GO:0006954)
regulation of B cell proliferation (GO:0030888)
antigen processing and presentation of exogenous peptide antigen (GO:0002478)
cytokine-mediated signaling pathway (GO:0019221)
antigen processing and presentation of exogenous peptide antigen via MHC class II (GO:0019886)
regulation of immune response (GO:0050776)
neutrophil mediated immunity (GO:0002446)
neutrophil degranulation (GO:0043312)
neutrophil activation involved in immune response (GO:0002283)
regulation of inflammatory response (GO:0050727)
positive regulation of response to external stimulus (GO:0032103)
regulation of smooth muscle cell migration (GO:0014910)
response to interferon-gamma (GO:0034341)
cytokine-mediated signaling pathway (GO:0019221)
cadmium ion transmembrane transport (GO:0070574)
response to cytokine (GO:0034097)
positive regulation of defense response (GO:0031349)
cellular response to tumor necrosis factor (GO:0071356)
cellular response to cytokine stimulus (GO:0071345)
membrane raft assembly (GO:0001765)
regulation of neutrophil extravasation (GO:2000389)
T cell extravasation (GO:0072683)
positive regulation of dendritic cell differentiation (GO:2001200)
regulation of neutrophil activation (GO:1902563)
intracellular sequestering of iron ion (GO:0006880)
positive regulation of neutrophil extravasation (GO:2000391)
left/right axis specification (GO:0070986)
antifungal humoral response (GO:0019732)
defense response to Gram-positive bacterium (GO:0050830)
Cluster 3
Cluster 2
Cluster 1
Cluster 0
-log (p value)

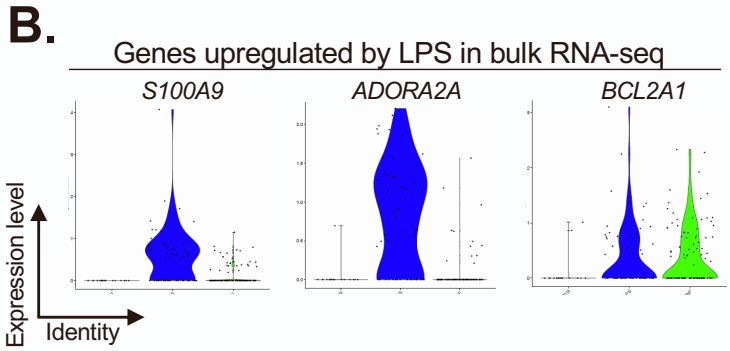
B.
Genes upregulated by LPS in bulk RNA-seq
S100A9
ADORA2A
BCL2A1
Expression level
Identity

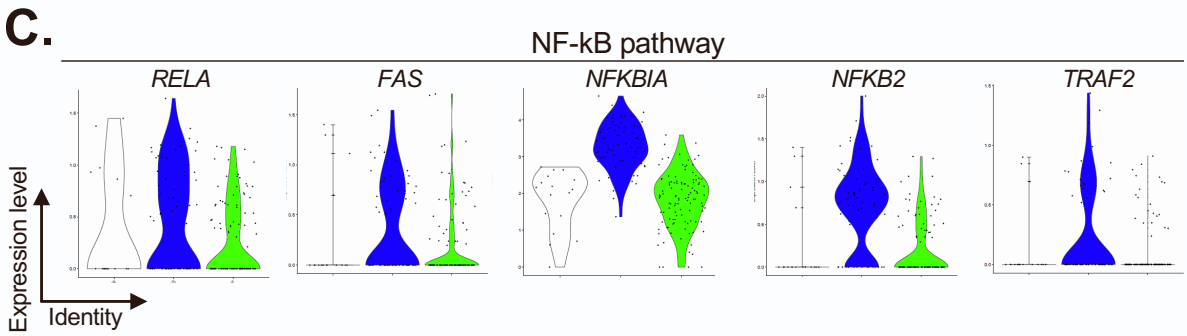
C.
NF-kB pathway
RELA
FAS
NFKBIA
NFKB2
TRAF2
Expression level
Identity

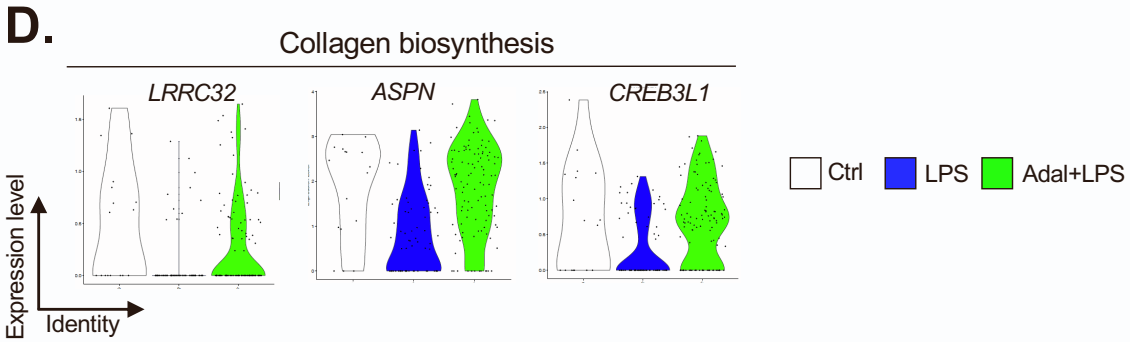
D.
Collagen biosynthesis
LRRC32
ASPN
CREB3L1
Expression level
Identity
Ctrl
LPS
Adal+LPS

Figure S10. [Similarities between GO terms and genes associated with AMC clusters and bulk RNA-seq analysis], Related to Figure 4. (A) UMAP plot of AMCs based on exposure as in Figure 4C is shown to facilitate visualization of the 4 clusters and their associated GO terms. (B-D) Violin plots for the key selected genes in different exposure groups of scRNA-seq AMC clusters were generated based on their differential regulation in the amnion bulk RNA-seq data.

Figure S11.

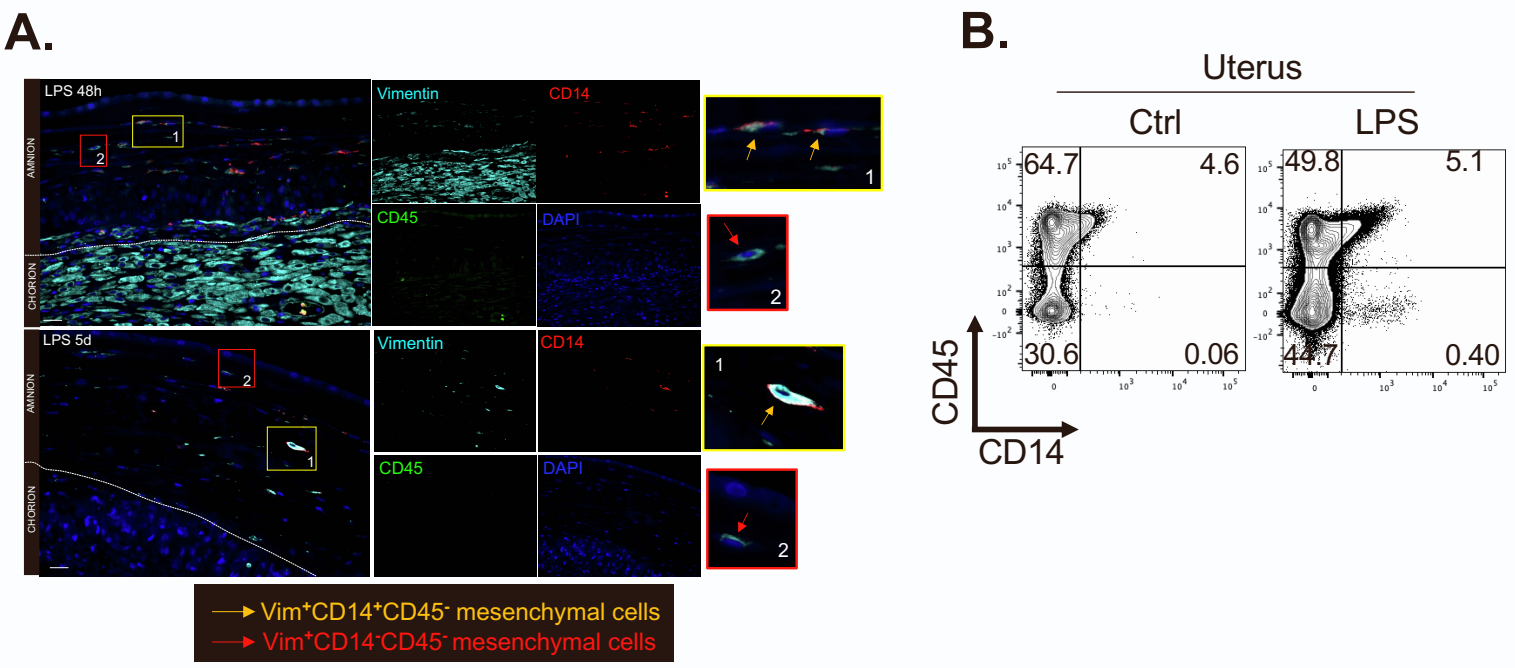

Figure S11. [Amnion Vim$^+$CD14$^-$CD45$^-$ cells persist 2d and 5d after LPS-exposure and low frequency of uterine CD14$^+$CD45$^-$ cells], Related to Figure 5. (A) Animals were delivered after a prolonged exposure to LPS for 48h or 5 days (5d). Rhesus chorioamnion-decidua section from paraffin-embedded blocks were stained with Vimentin (cyan), CD14 (red), CD45 (green), and DAPI (blue). Orange arrows in the magnified yellow insets (#1) indicate Vimentin(Vim)$^+$CD14$^+$CD45$^-$ cells, while red arrows in red insets (#2) indicate Vim$^+$CD14$^-$CD45$^-$ cells. Dotted white lines denote the different layers. Dotted white lines denote the different layers (amnion and chorion). Of note, Vim$^+$CD14$^+$CD45$^-$ were not present in the chorion layer. Representative sections (n=3/group) are shown. (B) Uterus of IA saline ctrl or LPS 16h animals was finely minced, digested, and cell suspension was analyzed by flow cytometry. Representative contour plots (n=2/treatment).

Figure S12.

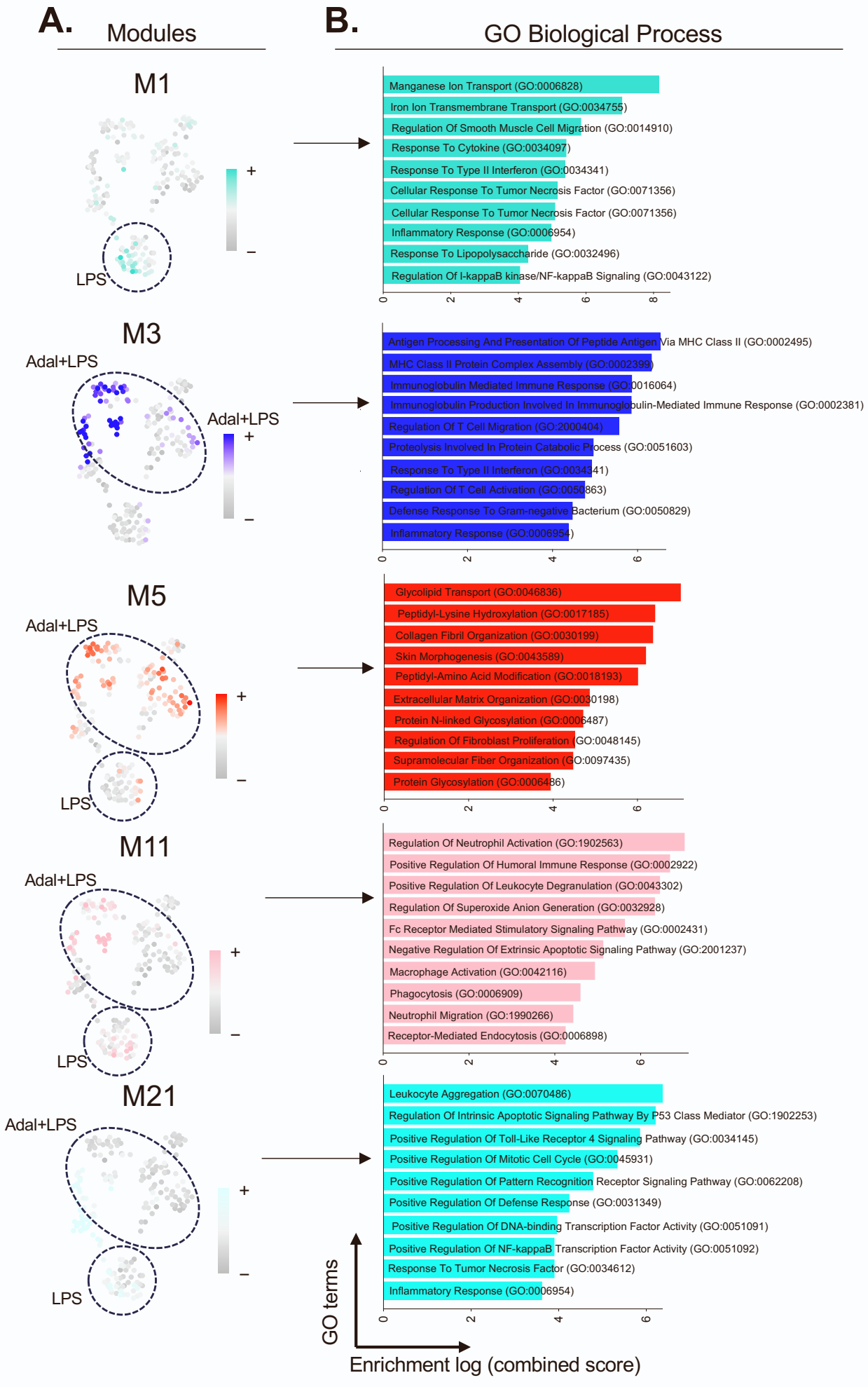
A.
Modules
B.
GO Biological Process
M1
LPS
+
–
Manganese Ion Transport (GO:0006828)
Iron Ion Transmembrane Transport (GO:0034755)
Regulation Of Smooth Muscle Cell Migration (GO:0014910)
Response To Cytokine (GO:0034097)
Response To Type II Interferon (GO:0034341)
Cellular Response To Tumor Necrosis Factor (GO:0071356)
Cellular Response To Tumor Necrosis Factor (GO:0071356)
Inflammatory Response (GO:0006954)
Response To Lipopolysaccharide (GO:0032496)
Regulation Of I-kappaB kinase/NF-kappaB Signaling (GO:0043122)
0
2
4
6
8
M3
Adal+LPS
Antigen Processing And Presentation Of Peptide Antigen Via MHC Class II (GO:0002495)
MHC Class II Protein Complex Assembly (GO:0002399)
Immunoglobulin Mediated Immune Response (GO:0016064)
Immunoglobulin Production Involved In Immunoglobulin-Mediated Immune Response (GO:0002381)
Regulation Of T Cell Migration (GO:2000404)
Proteolysis Involved In Protein Catabolic Process (GO:0051603)
Response To Type II Interferon (GO:0034341)
Regulation Of T Cell Activation (GO:0050863)
Defense Response To Gram-negative Bacterium (GO:0050829)
Inflammatory Response (GO:0006954)
0
2
4
6
M5
Adal+LPS
Glycolipid Transport (GO:0046836)
Peptidyl-Lysine Hydroxylation (GO:0017185)
Collagen Fibril Organization (GO:0030199)
Skin Morphogenesis (GO:0043589)
Peptidyl-Amino Acid Modification (GO:0018193)
Extracellular Matrix Organization (GO:0030198)
Protein N-linked Glycosylation (GO:0006487)
Regulation Of Fibroblast Proliferation (GO:0048145)
Supramolecular Fiber Organization (GO:0097435)
Protein Glycosylation (GO:0006486)
0
2
4
6
M11
Adal+LPS
Regulation Of Neutrophil Activation (GO:1902563)
Positive Regulation Of Humoral Immune Response (GO:0002922)
Positive Regulation Of Leukocyte Degranulation (GO:0043302)
Regulation Of Superoxide Anion Generation (GO:0032928)
Fc Receptor Mediated Stimulatory Signaling Pathway (GO:0002431)
Negative Regulation Of Extrinsic Apoptotic Signaling Pathway (GO:2001237)
Macrophage Activation (GO:0042116)
Phagocytosis (GO:0006909)
Neutrophil Migration (GO:1990266)
Receptor-Mediated Endocytosis (GO:0006898)
0
2
4
6
M21
Adal+LPS
Leukocyte Aggregation (GO:0070486)
Regulation Of Intrinsic Apoptotic Signaling Pathway By P53 Class Mediator (GO:1902253)
Positive Regulation Of Toll-Like Receptor 4 Signaling Pathway (GO:0034145)
Positive Regulation Of Mitotic Cell Cycle (GO:0045931)
Positive Regulation Of Pattern Recognition Receptor Signaling Pathway (GO:0062208)
Positive Regulation Of Defense Response (GO:0031349)
Positive Regulation Of DNA-binding Transcription Factor Activity (GO:0051091)
Positive Regulation Of NF-kappaB Transcription Factor Activity (GO:0051092)
Response To Tumor Necrosis Factor (GO:0034612)
Inflammatory Response (GO:0006954)
0
2
4
6
GO terms
Enrichment log (combined score)

Figure S12. [Co-expression network analysis of amnion mesenchymal cluster cells], Related to Figure 4. (A) scRNA-seq UMAP plots as in Figure 4C colored by module eigengenes (ME) for selected modules. Dotted line denotes clustering by prenatal treatments as in Figure 4C. (B) GO Biological Process enrichment analysis of the 100 most connected eigengenes for each module, as determined the eigengene-based connectivity (kME). Enriched terms are sorted by the combined Enrichr score. Only those modules with p-adjusted value<0.05 were retained.

Figure S13.

A.

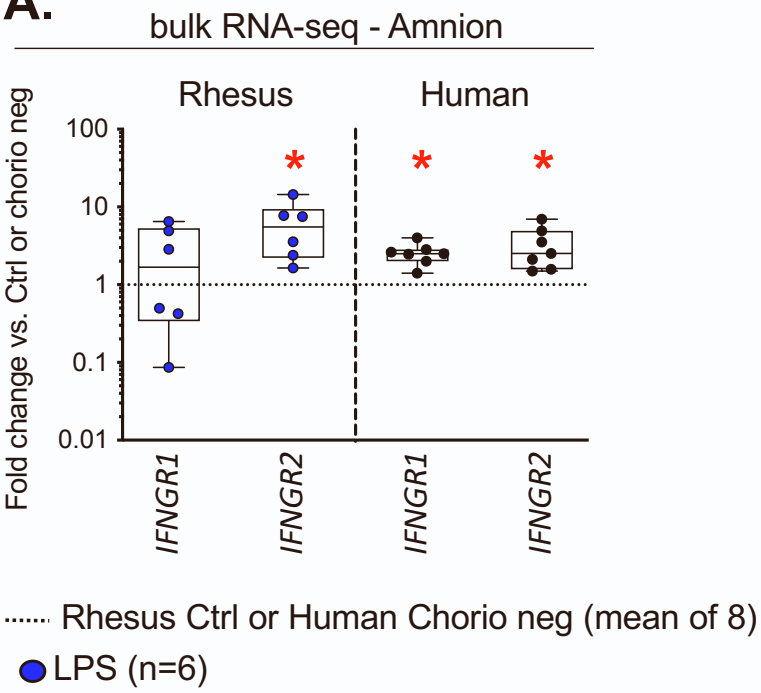

B.

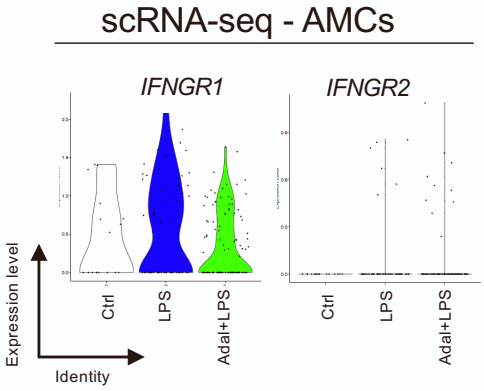

C.

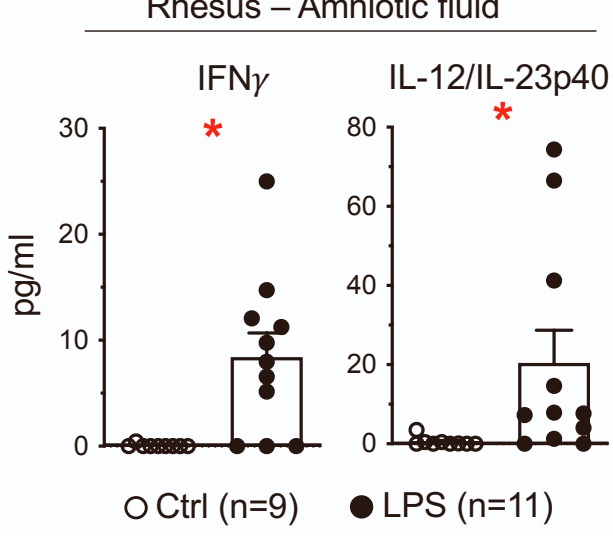

Figure S13. [Upregulation of IFNγ/IL12/IL23 axis upon exposure to LPS], Related to Figure 7. (A) Bulk RNA-seq analysis shows that inflammation induces a significant upregulation of *IFNGR1* (Interferon gamma receptor 1) in Rhesus and *IFNGR1* and *IFNGR2* (Interferon gamma receptor 2) transcripts in human amnion. (B) Similar results are observed with scRNA-seq of AMCs. (C) IFNγ and IL-12/IL-23p40 concentrations were measured in Rhesus amniotic fluid at delivery by Luminex using non-human primate multiplex kits (Millipore). Inflammation caused by LPS-exposure significantly increased the levels of these two cytokines that are characteristic of activated antigen presenting cells. Data are represented as mean±SE. P * <0.05 vs. ctrl in Rhesus or chorio neg in human (Mann–Whitney U test).